

Supramolecular architecture of metal-lustrous inclusion crystals based on aromatic CH– π interaction: versatile inclusion of 1-(*p*-ethoxyphenyl)-2-(2-thienyl)-5-[5-(tricyanoethenyl)-2-thienyl]pyrrole host with various electron-rich aromatic guest molecules

Rui Zhao,^a Shoji Matsumoto,^b Motohiro Akazome^b and Katsuyuki Ogura^{a,b,*}

^aGraduate School of Science and Technology, Chiba University, 1-33 Yayoicho, Inageku, Chiba 263-8522, Japan

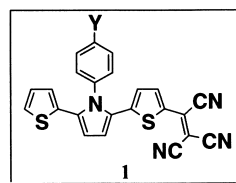
^bDepartment of Materials Technology, Faculty of Engineering, Chiba University, 1-33 Yayoicho, Inageku, Chiba 263-8522, Japan

Received 26 August 2002; accepted 18 October 2002

Abstract—1-(*p*-Ethoxyphenyl)-2-(2-thienyl)-5-[5-(tricyanoethenyl)-2-thienyl]pyrrole, a novel π -conjugated organic compound, shows particularly stronger affinities to various electron-rich aromatic guest molecules to form 2:1 inclusion complexes with gold- or bronze-like metallic luster. All of the complexes crystallize with the same so-called herringbone packing motif in which the π -system of the guest is sandwiched diagonally between the host molecules around it. The unique aromatic CH– π interactions between the host and the guest molecules essentially ascribe to the architecture of these complexes. The sidewise intermolecular π – π contacts (CN \cdots C=C) between the host molecules deeply affect the crystal appearance. © 2002 Published by Elsevier Science Ltd.

1. Introduction

Utilization of supramolecular architecture via non-covalent interactions is a vigorous field involving in the creation of new functional materials and is a powerful tool for particular structure formations.¹ Within the field of supramolecular chemistry, the non-covalent linkage of π -electron donating molecules to a π -deficient acceptor moiety through hydrogen bond and/or cooperative aromatic interactions² has attracted much attention in recent years. Recently, we have reported that 1-aryl-2-(2-thienyl)-5-[(5-tricyanoethenyl)-2-thienyl]pyrroles **1**, a new class of π -conjugated compounds consisting of a powerful π -electron withdrawing tricyanoethenyl substituent and a conjugated thiophene–pyrrole–thiophene skeleton, gives good-quality crystals with a gold- or bronze-like lustrous appearance.³ Furthermore, upon introduction of a heteroatom-combined methyl group such as OCH₃, SCH₃, or N(CH₃)₂ to the *para* position of the central *N*-phenyl group, **1** forms crystals with a brilliant red-violet metallic color which is obviously different from the other analogues (Scheme 1).⁴ X-Ray



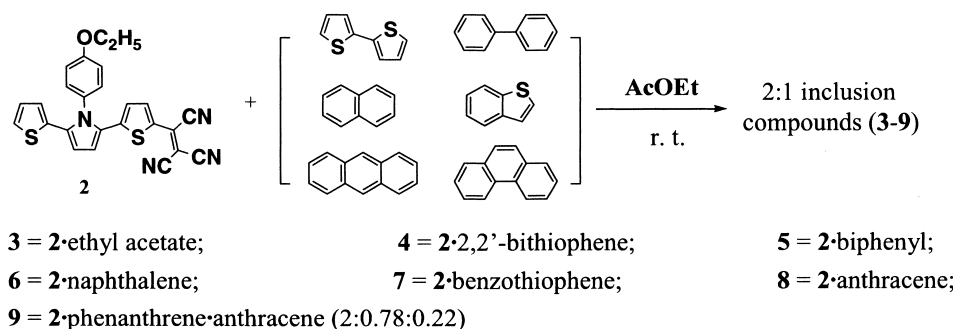
a: Y = OMe
b: Y = SMe
c: Y = NMe₂

Scheme 1. Structure of the 1-aryl-2,5-di(2-thienyl)pyrrole derivatives giving red–violet metallic colored crystals.

structural analysis revealed that the π -conjugated skeleton in these crystals adopts a heaving ribbon-like molecular arrangement and a weak CH/*n* type intramolecular hydrogen bond between the top of the cyano group and the heteroatom combined methyl group occurs to assist the formation of the wavy ribbon.⁴ In order to elucidate whether the methyl is essentially necessary to the special ribbon-like crystal arrangement or not, we designed compound **2** upon alteration of the substituent in the central *N*-phenyl ring of **1** to ethoxy group which is a bit longer than its methyl analogue. Beyond our estimation, the newly prepared derivative **2** does not crystallize from most of common organic solvents except for ethyl acetate. The gold-like crystals blending with a little black color, which crystallized from ethyl acetate at room temperature, were clarified as a 2:1 complex of **2** with the solvent molecules by ¹H NMR and X-ray analysis. Against this background, we envisaged that complexation of a suitable guest to **2** may be a

Keywords: π -conjugated organic compound; electron-rich aromatic guest molecule; inclusion complex; gold or bronze-like metallic luster; aromatic CH– π interaction; sidewise intermolecular π – π contacts (CN \cdots C=C).

* Corresponding author. Address: Department of Materials Technology, Faculty of Engineering, Chiba University, 1-33 Yayoicho, Inageku, Chiba 263-8522, Japan. Tel.: +81-43-290-3388; fax: +81-43-290-3402; e-mail: katsu@galaxy.tc.chiba-u.ac.jp



Scheme 2. Complexation of 1-(*p*-ethoxyphenyl)-2-(2-thienyl)-5-[5-(tricyanoethenyl)-2-thienyl]pyrrole with ethyl acetate and some electron-rich aromatic guests.

necessary condition concerning its crystallinity. Since **2** bears an electron-withdrawing tricyanoethenyl group, we made use of various electron-rich aromatic guests such as 2,2'-bithiophene, benzothiophene, biphenyl, naphthalene, anthracene, and phenanthrene in ethyl acetate solution to inspect their complexation behavior (Scheme 2). Here we describe the preparation, thermal stability, solid-state UV–Vis–NIR diffuse reflection–absorption spectra, and X-ray structures of the π -complexes of **2** with the electron-rich aromatic guests.

2. Results and discussion

2.1. Preparation of the inclusion crystals

The title host compound **2** was synthesized by a method analogous to the procedures we have reported.³ Inclusion compounds **3–8** were prepared by simple crystallization of

2 together with an excess amount of the respective guest compounds from their ethyl acetate solution. We also tried to grow the inclusion crystals by employing chloroform as solvent, but failed in formation of crystals with good quality. Preparation of single crystals of complex **9** containing mixed guests of anthracene and phenanthrene is given below. The common stoichiometric ratio in these crystalline inclusions is 2:1 (host/guest).

2.2. X-Ray structural studies

Firstly, we studied the crystal structure of the ethyl acetate-included complex **3**. The X-ray analysis discloses that self-association of the four neighboring host molecules creates a sheet possessing two kinds of cavities. The ethyl acetate guest is trapped in one of the host-surrounded cavities to form the cocrystal **3**, and the other half of the cavities is filled up naturally by the *p*-ethoxyphenyl group above or below the basic sheet, as shown in Fig. 1. In this complex,

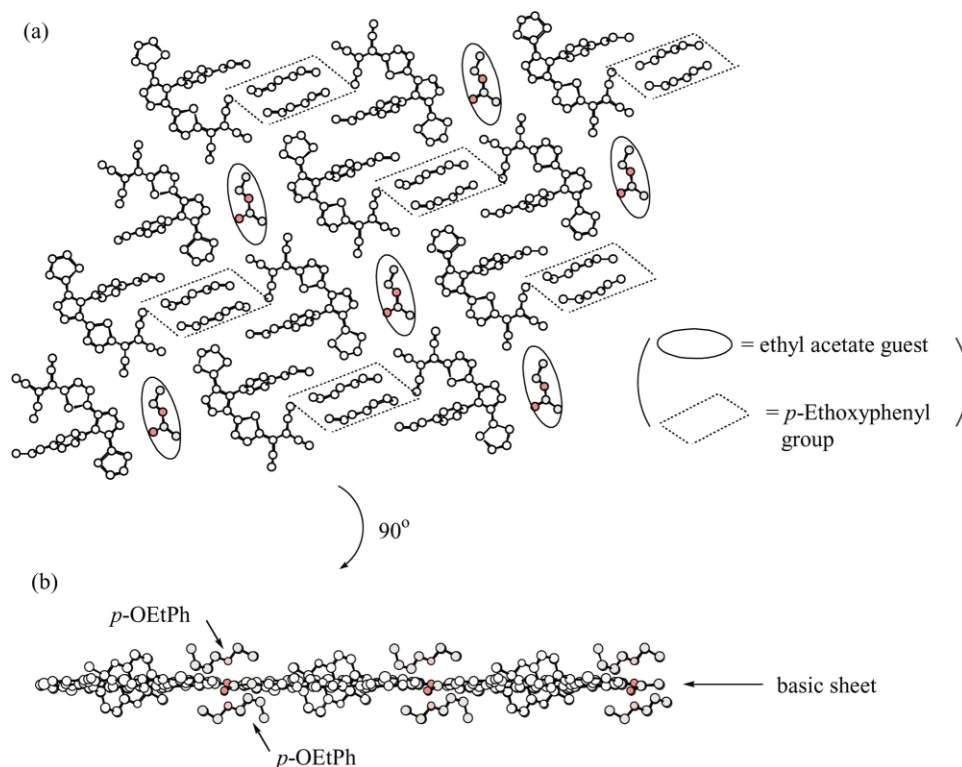


Figure 1. Crystal arrangement of complex **3**. Hydrogen atoms are omitted for clarity. (a) Top view of the sheet-like structure. The host-surrounded cavities filled up by ethyl acetate guest and *p*-ethoxyphenyl group are marked with elliptical and square signs, respectively. (b) Side view of the sheet-like structure.

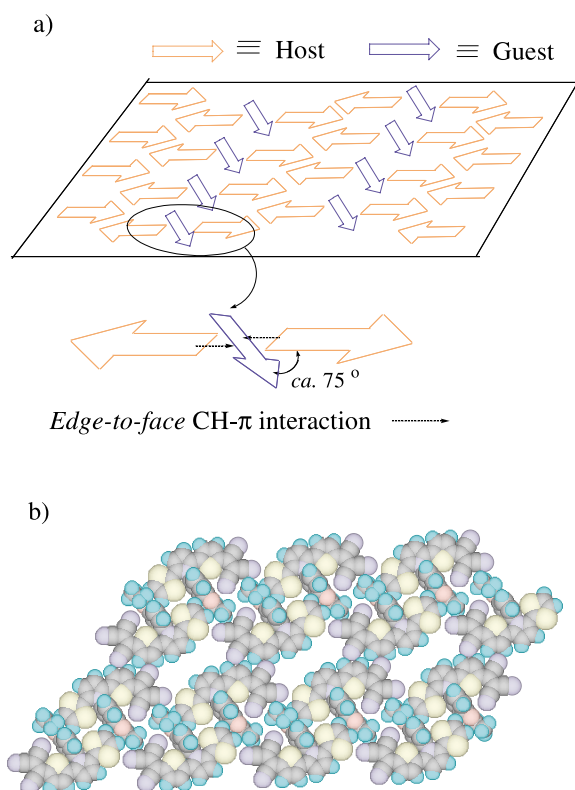


Figure 2. (a) Crystal arrangement and basic packing motif of the inclusion compounds **4–9**. The edge-to-face CH- π interaction is represented with dotted arrows; (b) space-filling packing of a guest-omitted sheet, showing the open cavities.

the guest molecules are fixed by a stronger hydrogen bond ($-\text{OC}=\text{O} \cdots \text{H}-\text{C}=\text{C}$: 2.26 Å (159.6°)) between the carbonyl oxygen (guest) and the olefinic hydrogen on the central pyrrole ring (host).

The inclusion crystals of **4–9** are isostructural and crystallize in the same space group $P\bar{1}$, and the electron-rich aromatic guest molecules lie in cavities on the sheets formed by self-association of the planar π -system of the host **2**. The basic packing motif of these π -complexes is the so-called herringbone style which is very similar to that of naphthalene, as indicated by Gavezzotti who carried out a very comprehensive study of the packing patterns of planar aromatic hydrocarbons.⁵ The aromatic guest is sandwiched diagonally between the host molecules around it, giving a host-guest interplanar angle of ca. 75°, which is favorable to generate an edge-to-face aromatic CH- π interaction, as illustrated schematically in Fig. 2.

As a typical example, the crystal structure of 2,2'-bithiophene included complex **4** is illustrated in detail. The unit cell contains two parallel molecules of host **2** and one molecule of 2,2'-bithiophene which is sandwiched diagonally between the two parallel hosts with a dihedral angle of ca. 75° (Fig. 3(a)). The host molecule **2** interacts with the adjacent one through the sidewise intermolecular π - π contacts ($\text{CN} \cdots \text{C}=\text{C}$) to give a somewhat warped sheet and form host tetramer-surrounded cavities in which the 2,2'-bithiophene guest is sandwiched (Fig. 3(b) and (c)). The cavity is found to have approximate dimensions of

12.14 \times 5.67 Å, corresponding to the interatomic distance of $\text{N39} \cdots \text{N38}^\ddagger$ and $\text{H24} \cdots \text{H17}^\ddagger$, respectively, as mapped by a Cambridge crystal packing program.[§] The warped sheet stacks to produce a basic crystal skeleton and the guest enters the spaces (cavities) through the stacked sheets with a regular alternation manner to construct the inclusion crystal (Fig. 3(d)). The $\text{CN} \cdots \text{C}=\text{C}$ contacts ($\text{N38} \cdots \text{C14}$: 3.55 Å; $\text{N38} \cdots \text{C19}$: 3.46 Å; $\text{N39} \cdots \text{C30}$: 3.58 Å) between the adjacent host molecules are suggested to be responsible for the gold-like metallic luster of the inclusion crystals (Fig. 3(c) and Table 1).³ The edge-to-face aromatic CH- π interactions⁶ between the two olefinic C-H groups of the central pyrrole ring of host **2** and two aromatic ring centers (2-thienyl group on left and right side, i.e. ring A and B in Fig. 3(c)) of 2,2'-bithiophene are found to have relatively longer^{6a} C-H \cdots i (thienyl centroid) distance of 3.080 Å with C-H \cdots i angle of 132.6° and 2.809 Å (141.2°), corresponding to C-H1 \cdots i_A and C-H2 \cdots i_B, respectively (Fig. 3(c) and Table 1). The C-H \cdots S contacts⁷ are 3.05 Å with a C-H \cdots S angle of 141.6° and 3.04 Å (148.7°), corresponding to C-H1 \cdots S_A and C-H2 \cdots S_B, respectively. Allowing for that the π -electron dispersion is not so uniform, that is, the electron cloud is relatively denser on sulfur atom of the thienyl group, we envisage that the C-H \cdots S interaction is more approximate to reflect the true magnitude of the CH- π interaction in complex **4**. Detailed information of the aromatic CH- π interaction of these supramolecular assemblies are listed in Table 1.[¶] The edge-to-face type aromatic interaction (T-shaped π - π stacking) has been reported as the most stable geometry between the two aromatic rings in a large number of papers.^{6c,8} Unlike the channel-possessed inclusion compound which usually makes guest molecules stack,⁹ there is no evident guest-guest contact in crystals **4–9**.

Interestingly, the crystal appearance shows delicate changes with the alteration of the guest molecules. Complex **4**, **6**, and **7** give brilliant gold-like lustrous crystals; complex **5** form crystals with a medium metallic color between gold-like and bronze-like; complex **8** and **9** show bronze-like metallic luster which essentially differs from those mentioned above. It seems that the appearance of the complex containing smaller guest molecule is closer to the gold-like metallic color, whereas those including larger guest resemble better in the bronze-like metallic luster. We have demonstrated that the π -conjugated system of most of analogues of **2** adopts a coplanar sheet-like molecular arrangement and the interatomic contacts between the cyano group and the olefinic carbon ($\text{CN} \cdots \text{C}=\text{C}$) play an important role in the gold-like appearance that the crystals show. Such $\text{CN} \cdots \text{C}=\text{C}$ contact in complexes **4–9** is found to occur possibly in three places, as shown in Fig. 4. When a relatively smaller guest is included, that is, the four adjacent

[†] Symmetry operation used to generate the atoms of neighboring unit: $-x-1, -y-1, -z+2$.

[‡] Symmetry operation: $-x+3, -y+1, -z+2$.

[§] CS Chem3D Pro ver. 5.0 produced by Cambridge Soft Corporation, USA, 1999.

[¶] The C-H bond lengths applied to the calculation of the d value are based on the results of X-ray structural analysis and not normalized to the neutronographic value which has been reported as 1.083 Å and used in the correlated calculation of edge-to-face type aromatic CH- π interaction.^{6a}

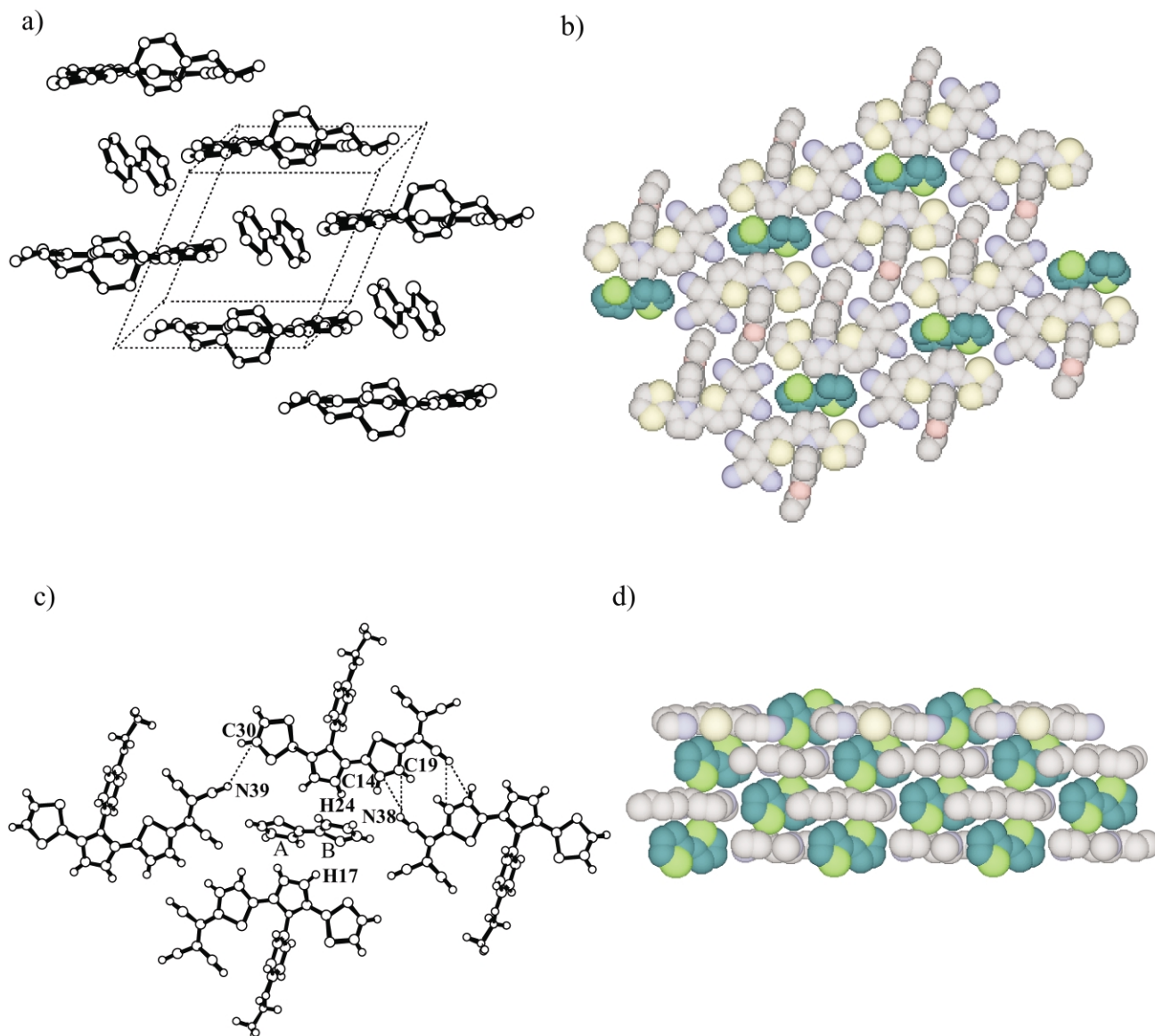


Figure 3. Packing diagram of complex **4**. Unnecessary H atoms are omitted. (a) Molecular arrangement in the unit cell; (b) space-filling packing of the sheet-like structure; (c) sidewise π - π contacts (CN \cdots C=C) among the adjacent host molecules: N38 \cdots C14: 3.55 Å (C-H \cdots N angle 103.1°); N38 \cdots C19: 3.46 Å (115.2°); N39 \cdots C30: 3.58 Å (114.4°), and the edge-to-face CH- π interactions between the host C-H groups and aromatic ring A and B of the guest. The interatomic distance of N39 \cdots N38 (12.14 Å) and H24 \cdots H17 (5.67 Å) determine the cavity's approximate dimensions; (d) space-filling packing of the whole crystal. Some parts of the host atom are omitted to clearly show the general arrangement of guest molecules.

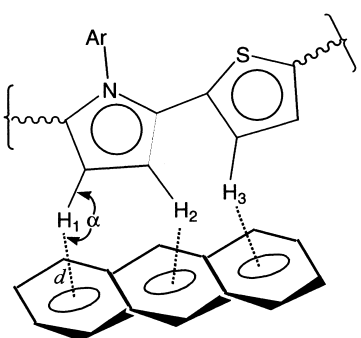
host molecules surround a not so large cavity, all the three interactions a, b, and c can occur simultaneously; with the increasing volume of the guest, the cavity length must get longer enough, and this makes the CN \cdots C=C contacts a and b become weaker and weaker, even disappear at last if the guest is large enough; in contrast to a and b which deeply concern the cavity length l , interaction c is hardly affected by the guest size change, hence, remains as the only contact between the adjacent hosts.¹¹ Therefore, complex **4**, **6** and **7** that are able to keep on all the three possible contacts, form almost the same gold-like crystals; the other complexes, beginning from **5**, deviate from the gold-like metallic luster gradually, and at last, the largest guests-included complexes **8** and **9** completely change their appearance to bronze-like.

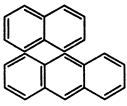
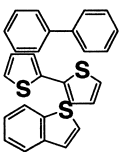
¹¹ The CN \cdots C=C contact shown in Fig. 4 is difficult to give a definite judgment because of the somewhat disordered terminal thiophene ring.

The relationship between the crystal appearance and the CN \cdots C=C contact together with the cavity length l is summarized in Table 2. This tendency is also reflected in the solid state UV-Vis-NIR diffuse reflection-absorption spectra of the complexes (Fig. 5).

2.3. Solid-state UV-Vis-NIR diffuse reflection-absorption spectra

Following our previous study,³ the solid-state UV-Vis-NIR diffuse reflection-absorption spectra of these inclusion crystals again display a peculiar broadened absorption band in the whole visible region (Fig. 5), reflecting the shorter contacts among the host π -electron systems are widespread within all crystal lattice of the complexes. For the gold-like complexes **4**, **6**, and **7**, the λ_{\max} of absorption bands on the visible region lies in a narrow range of 480–490 nm,

Table 1. Aromatic CH– π interaction parameters in inclusion compound 4–9


Guest	d (Å) ^a	α (deg.) ^a	
	C–H1	2.876	140.4
	C–H2	2.647	140.2
	C–H1	2.936	139.4
	C–H2	2.611	131.4
	C–H3	3.000	141.0
	C–H1	3.070	149.4
	C–H2	2.756	170.8
	C–H1	3.080	132.6
	C–H2	2.809	141.2
	_{-b}	_{-b}	_{-b}

^a The distance d is taken to the aromatic ring centroid (i) of guest molecule and α is the (C–H... i) angle.

^b Cannot be determined precisely because of the disordered benzothio-phenylene guest.

corresponding to the greenish blue light. For complex **5**, its λ_{\max} slightly shifts to the longer wavelength of about 510 nm. The bronze-like complexes **8** and **9** once more give rise to their λ_{\max} of visible region absorptions at about 540 nm. It is not surprised that the difference in the absorption bands is really subtle because all of the complexes are isostructural, but such discrimination exactly reflects that the CN...C=C contacts among the host molecules is not in the same level, which essentially determines the metallic color of the cocrystals 4–9. The appearance of the absorption bands at a longer wavelength within the near-infrared region is almost identical with each other.

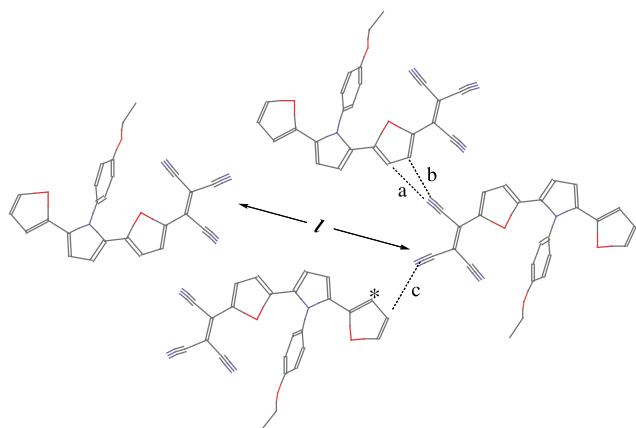


Figure 4. Three possible intermolecular π – π contacts (CN...C=C) among the host molecules within the sheet of π -complexes 4–9. Length of the open cavity is represented by l , and the related carbon atom on the somewhat disordered terminal thiophene ring is marked with a star symbol. H atoms are omitted for clarity.

Table 2. CN...C=C contacts, cavity length and crystal appearance of complexes 4–9

Complex	CN...C=C interaction (Å)			Cavity length l (Å)	Crystal appearance
	a	b	c		
7	3.46	3.51	3.52	11.24	Gold-like
6	3.51	3.48	3.49	11.45	Gold-like
4	3.55	3.46	3.58	12.14	Gold-like
5	4.51	3.97	3.67	13.08	Medium
8	4.94	4.20	3.62	13.51	Bronze-like
9	5.00	4.39	3.63	13.32	Bronze-like

2.4. Inclusion competition between anthracene and phenanthrene guests

During this study, we found that the phenanthrene guest cannot be included directly under the standard experimental conditions. In this case, the ethyl acetate solvent molecule is included exclusively instead of phenanthrene. We surmise that the molecular height of phenanthrene is possibly responsible for the low inclusion ability because the central C=C bond does not lie in a horizontal position with the fused left and right aromatic rings, which is an significant point for formation of a uniform host–guest CH– π interaction. By accident, we directly used some unrefined ethyl acetate solvent mixed with a small amount of anthracene (concentration unknown) to prepare the complex of 2-phenanthrene. To our surprise, single crystals with mixed guests of anthracene (**A**) and phenanthrene (**P**) were obtained (complex **9**). ¹H NMR spectrum showed that **9** included 39% **P** and 11% **A** (as mole percentages). We elucidated the structure of **9** by X-ray analysis and found that **9** is also isostructural with the other complexes. However, the Fourier map obtained after the host structure had been refined could only be interpreted as a severely disordered guest, an average of **A** and **P**.¹⁰ We therefore carried out a competition experiment between **A** and **P** guests by dissolving compound **2** in the ethyl acetate solution mixed with **A** and **P** (total 1.6 equiv. to **2**) in different proportions. The results (Fig. 6, drawn as quadrilateral marker) determined by ¹H NMR demonstrate that the inclusion ability of **A** is exceedingly higher than **P**.

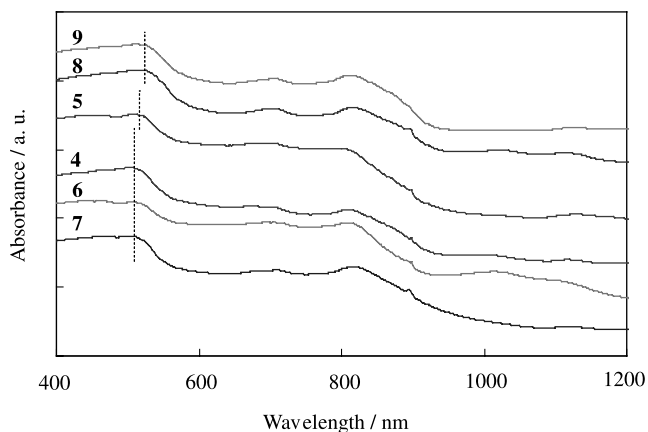


Figure 5. Solid-state UV–Vis–NIR absorption spectra of the inclusion crystals 4–9. The λ_{\max} of absorption bands on the visible region is: 480–490 nm for **4**, **6** and **7**, 510 nm for **5**, and 540 nm for **8** and **9**.

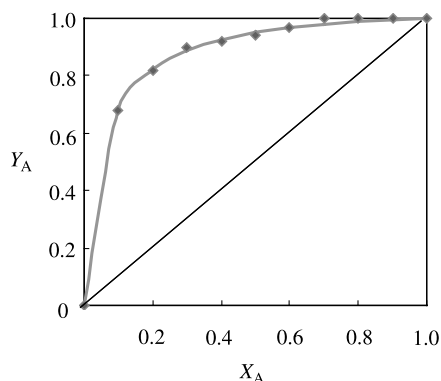


Figure 6. Optimum curve (drawn as gray solid line, simulated by using least square fitting) and experimental results (drawn as quadrilateral marker) of the inclusion competition between anthracene (**A**) and phenanthrene (**P**) guests. X_A is the mole fraction of **A** guest in solution; Y_A is the mole fraction of **A** guest in crystal.

Based on the experimental results, we simulated the optimum curve (Fig. 6, drawn as gray solid line) of this competition by applying the least square fitting to the correlated calculation and concluded that the inclusion ability of **A** is 18.9 times higher than **P**. This again proves that whether a uniform host–guest CH– π interaction can be smoothly generated or not virtually determines the inclusion crystal formation.

2.5. Thermal analysis

The thermal gravimetry (TG) and differential scanning calorimetry (DSC) traces for the inclusion compounds **3–8** are shown in Fig. 7. The ethyl acetate-included complex **3** decomposes in a single step in the weight loss curve, and the DSC shows a first endotherm due to guest loss, followed by a sharp endotherm due to the host melt. The crystal of complex **3** entirely releases the ethyl acetate guest at 102.6°C, which is much higher than the boiling point of ethyl acetate (77°C). This indicates that the guest release from the cavities is probably affected not only by the host–guest hydrogen bonding, but also by a steric hindrance which is induced by the crystalline matrix. A similar result had been observed and interpreted by Apel et al., who made

use of 4,4'-(fluorene-9,9-diyl)diphenol as host molecule in their host–guest inclusion studies.¹¹ The weight loss data derived from the TG trace for **3** is in good agreement with the stoichiometric ratio (2:1). Complex **5–7** decompose at 166.9, 165.8 and 157.6°C, respectively, and the endotherms corresponding to the host melt appear as sharply and obviously as that of the complex **3** because the guests evaporate rapidly with the temperature rising after the complexes decomposed. As to the complex **4** and **8** that include nonvolatile guests, the host melt endotherm does not appear because of the guest dissolution in the host.¹² The complete decomposition temperature of the two complexes rises up gradually from 189.2 to 196.6°C, corresponding to complex **4** and **8**, respectively. It is evident that the thermal stability of these complexes increases with the increasing electron density of the guest π -system. Combined with the fact that the electron-deficient 2,2'-bipyridine cannot be included because its electronic property is unfavorable to the electrostatic interaction between the host and the guest π -system, we can infer that electrostatic force also play a role in these supramolecular architecture and is the major factor determining the stability of the complexes.¹³

3. Conclusion

As described above, inclusion of electron-rich aromatic molecules with the host compound **2** bearing a stronger electron-withdrawing tricyanoethenyl group leads to the formation of a series of π -complexes with a same stoichiometric ratio of 2:1 (host/guest). These inclusion crystals show gold- or bronze-like metallic luster, which is much rare in supramolecular chemistry. The crystals of the complexes **4–9** are isostructural and crystallize in same space group $P\bar{1}$ with a basic packing motif of the so-called herringbone style. The host molecule **2** interacts with the adjacent one through the intermolecular π – π contacts (CN $\cdot\cdot$ C=C) to give a not strictly planar sheet and result in host tetramer-surrounded cavities in which the aromatic guest is sandwiched diagonally, giving a host–guest interplanar angle of ca. 75°. This pattern is favorable to generate an type aromatic CH– π interaction which is suggested to be essentially contributable to the architecture

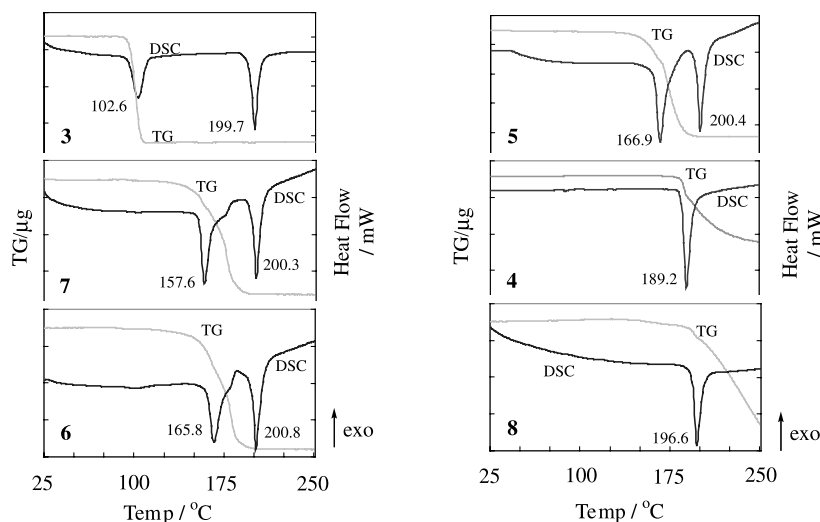
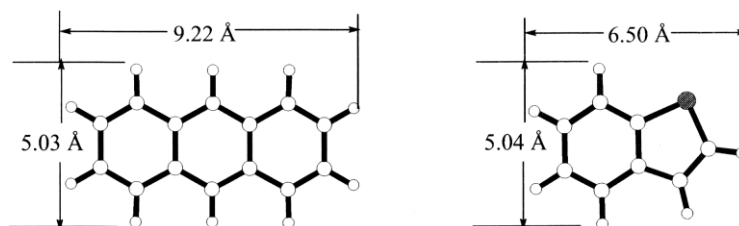


Figure 7. Thermograms (TG and DSC) of the inclusion compound **3–8**. The complex number is represented with bold Arabic numerals.



Scheme 3. Molecular size of anthracene and benzothiophene calculated by MM2 method.

of these π -complexes. The crystal appearance shows delicate changes with the alteration of the guest molecules, which is interpreted finally as the alteration of the sidewise intermolecular π - π contacts ($\text{CN}\cdots\text{C}=\text{C}$) between the host molecules. The thermal stability of these complexes increases with the increasing electron density of the guest π -system, suggesting that electrostatic force also play a role in these supramolecular architecture and is the major factor determining the stability of the complexes.

Actually, the guest molecules applied in this work are in a considerably wide range. Besides those mentioned above, we also tested the inclusion possibility of other aromatic molecules such as thiophene, [2,2';5,2'']terthiophene, *p*-terphenyl, naphthalene, and bis(ethylenedithio)-tetrathiafulvalene. Except that [2,2';5,2'']terthiophene is included to form a bronze-like metallic colored complex with a host/guest ratio of 2:1, the others are all failed in inclusion, and unfortunately, the satisfactory structure analysis of the [2,2';5,2'']terthiophene-included crystal has not been obtained till now. There is no problem in the electronic property of the newly applied guest molecules because they all show good electrostatic complementarity with host **2**, just like the successfully included guests we introduced. The only key point that may be considered here is the molecular size. Compared with the guests in complexes **4–9**, they are too small or too large to be located in the cavities formed by self-association of the host **2**. In spite of the unknown structure of the [2,2';5,2'']terthiophene included crystal, we suggest that the ideal guest size suitable for inclusion is not strictly limited in a range of 6.50–9.22 Å in length, and less than 5.04 Å in height.** (Scheme 3).

4. Experimental

4.1. General methods

All chemicals were obtained from commercial suppliers and used without further purification. ^1H NMR spectra were recorded at 300 MHz using a varian Gemini-2000 NMR spectrometer and chemical shifts were referenced to TMS as internal standard. Thermal Analyses (TG-DSC) were

** The precise molecular dimension of benzothiophene guest cannot be measured directly from the result of X-ray structural analysis because of its disordered conformation. To standardize the result, we used MM2 calculation program to approach the correct conformation of anthracene and benzothiophene and measured the two dimensions based on the calculated results. The actual dimension of anthracene determined by X-ray structural analysis in this work is 4.75×9.06 Å, which is slightly deviated from the calculated result.

carried out on a Mac science TG-DSC3100s apparatus. The measurements were performed over the temperature range 25–250°C at a heating rate of $10^\circ\text{C min}^{-1}$ with a purge of dry nitrogen flowing at the pressure of ca. 0.15 MPa. UV-Vis absorption spectra in THF solution were recorded on a JASCO V-570 spectrophotometer. Solid-state UV-Vis-NIR diffuse reflection-absorption spectra were recorded on a JASCO V-570 spectrophotometer equipped with an integral detector. Single crystals of the corresponding compounds were uniformly broken into powder and were put into a quartz glass cell for measurement under the absorption response mode. Infrared spectra were measured on a JASCO FT/IR-350 spectrophotometer. Melting points are uncorrected. Elemental analyses were performed by Chemical Analysis Center of Chiba University.

4.2. Materials

The host compound **2** and its precursor **1** were prepared according to the literature procedures we have published.^{3,14}

4.2.1. 1-(*p*-Ethoxyphenyl)-2,5-di(2-thienyl)pyrrole. Pale yellow needles; mp 157.5–159.5°C; ^1H NMR (300 MHz, CDCl_3) δ 1.46 (t, $J=7.0$ Hz, 3H), 4.08 (q, $J=7.0$ Hz, 2H), 6.53 (s, 2H), 6.58 (dd, $J=1.1, 3.7$ Hz, 2H), 6.82 (dd, $J=3.7, 5.1$ Hz, 2H), 6.93 (d, $J=8.9$ Hz, 2H), 7.04 (dd, $J=1.1, 5.1$ Hz, 2H), 7.22 (d, $J=9.1$ Hz, 2H); IR (KBr) 1514, 1413, 1292, 1248, 1198, 1169, 1115, 1047, 833, 762, 702 cm^{-1} . Anal. calcd for $\text{C}_{20}\text{H}_{17}\text{NOS}_2$: C, 68.34; H, 4.88; N, 3.99. Found: C, 68.32; H, 4.84; N, 3.97.

4.2.2. 1-(*p*-Ethoxyphenyl)-2-(2-thienyl)-5-[5-(tricyanoethenyl)-2-thienyl]pyrrole(2). Gold-like metallic colored fine powders; mp 201.2–201.9°C; ^1H NMR (300 MHz, CDCl_3) δ 1.49 (t, $J=7.0$ Hz, 3H), 4.13 (q, $J=7.0$ Hz, 2H), 6.74 (d, $J=4.3$ Hz, 1H), 6.86 (dd, $J=1.2, 3.7$ Hz, 1H), 6.91 (dd, $J=3.8, 5.1$ Hz, 1H), 7.07 (d, $J=4.3$ Hz, 1H), 7.08 (d, $J=8.9$ Hz, 2H), 7.09 (d, $J=4.7$ Hz, 1H), 7.17 (dd, $J=1.2, 5.1$ Hz, 1H), 7.30 (d, $J=8.9$ Hz, 2H), 7.74 (d, $J=4.5$ Hz, 1H); IR (KBr) 2210, 1510, 1452, 1425, 1402, 1250, 1182, 1111, 1063, 845 cm^{-1} ; UV-Vis (THF, 3×10^{-5} M) λ_{max} (nm) (ϵ ($\text{M}^{-1} \text{cm}^{-1}$)) 638 (48000). Anal. calcd for $\text{C}_{25}\text{H}_{16}\text{N}_4\text{OS}_2$: C, 66.35; H, 3.56; N, 12.38. Found: C, 66.10; H, 3.53; N, 12.30.

4.2.3. 1-(*p*-Ethoxyphenyl)-2-(2-thienyl)-5-[5-(tricyanoethenyl)-2-thienyl]pyrrole-ethyl acetate complex (3). Gold-like lustrous crystals; dec (TG-DSC) 102.6°C; ^1H NMR (300 MHz, CDCl_3) δ 1.26 (t, $J=7.2$ Hz, 1.5 H), 1.49 (t, $J=7.0$ Hz, 3H), 2.05 (s, 1.5H), 4.12 (q, $J=7.0$ Hz, 1H), 4.13 (q, $J=7.0$ Hz, 2H), 6.74 (d, $J=4.3$ Hz, 1H), 6.86 (dd,

$J=1.2, 3.7$ Hz, 1H), 6.91 (dd, $J=3.8, 5.1$ Hz, 1H), 7.07 (d, $J=4.3$ Hz, 1H), 7.08 (d, $J=8.9$ Hz, 2H), 7.09 (d, $J=4.7$ Hz, 1H), 7.17 (dd, $J=1.2, 5.1$ Hz, 1H), 7.30 (d, $J=8.9$ Hz, 2H), 7.74 (d, $J=4.5$ Hz, 1H); IR (KBr) 2208, 1730, 1498, 1421, 1398, 1362, 1250, 1182, 1111, 845 cm^{-1} . Anal. calcd for $2\text{C}_{25}\text{H}_{16}\text{N}_4\text{OS}_2\cdot\text{C}_4\text{H}_8\text{O}_2$: C, 65.30; H, 4.06; N, 11.28. Found: C, 65.34; H, 4.12; N, 11.23.

4.2.4. 1-(*p*-Ethoxyphenyl)-2-(2-thienyl)-5-[5-(tricyanoethenyl)-2-thienyl]pyrrole-2,2'-bithiophene complex (4). Gold-like lustrous crystals; dec (TG-DSC) 189.2°C; ^1H NMR (300 MHz, CDCl_3) δ 1.49 (t, $J=7.0$ Hz, 3H), 4.13 (q, $J=7.0$ Hz, 2H), 6.74 (d, $J=4.3$ Hz, 1H), 6.86 (dd, $J=1.2, 3.7$ Hz, 1H), 6.91 (dd, $J=3.8, 5.1$ Hz, 1H), 7.02 (dd, $J=3.6, 5.1$ Hz, 1H), 7.07 (d, $J=4.3$ Hz, 1H), 7.08 (d, $J=8.9$ Hz, 2H), 7.09 (d, $J=4.7$ Hz, 1H), 7.17 (dd, $J=1.2, 5.1$ Hz, 1H), 7.18 (dd, $J=1.2, 3.6$ Hz, 1H), 7.21 (dd, $J=1.2, 5.1$ Hz, 1H), 7.30 (d, $J=8.9$ Hz, 2H), 7.74 (d, $J=4.5$ Hz, 1H); IR (KBr) 2208, 1498, 1450, 1421, 1396, 1362, 1244, 1165, 1107, 1065, 845 cm^{-1} . Anal. calcd for $2\text{C}_{25}\text{H}_{16}\text{N}_4\text{OS}_2\cdot\text{C}_8\text{H}_6\text{S}_2$: C, 65.02; H, 3.57; N, 10.46. Found: C, 64.77; H, 3.66; N, 10.40.

4.2.5. 1-(*p*-Ethoxyphenyl)-2-(2-thienyl)-5-[5-(tricyanoethenyl)-2-thienyl]pyrrole-biphenyl complex (5). Golden yellow crystals; dec (TG-DSC) 168.0°C; ^1H NMR (300 MHz, CDCl_3) δ 1.49 (t, $J=7.0$ Hz, 3H), 4.13 (q, $J=7.0$ Hz, 2H), 6.74 (d, $J=4.3$ Hz, 1H), 6.86 (dd, $J=1.2, 3.7$ Hz, 1H), 6.91 (dd, $J=3.8, 5.1$ Hz, 1H), 7.07 (d, $J=4.3$ Hz, 1H), 7.08 (d, $J=8.9$ Hz, 2H), 7.09 (d, $J=4.7$ Hz, 1H), 7.17 (dd, $J=1.2, 5.1$ Hz, 1H), 7.30 (d, $J=8.9$ Hz, 2H), 7.36 (dd, $J=1.5, 8.4$ Hz, 1H), 7.45 (tt, $J=1.5, 8.4$ Hz, 2H), 7.60 (dt, $J=1.5, 8.4$ Hz, 2H), 7.74 (d, $J=4.5$ Hz, 1H); IR (KBr) 2208, 1508, 1421, 1396, 1362, 1246, 1182, 1107, 1070, 856 cm^{-1} . Anal. calcd for $2\text{C}_{25}\text{H}_{16}\text{N}_4\text{OS}_2\cdot\text{C}_{12}\text{H}_{10}$: C, 70.30; H, 4.00; N, 10.58. Found: C, 70.10; H, 4.04; N, 10.52.

4.2.6. 1-(*p*-Ethoxyphenyl)-2-(2-thienyl)-5-[5-(tricyanoethenyl)-2-thienyl]pyrrole-naphthalene complex (6). Gold-like lustrous crystals; dec (TG-DSC) 166.1°C; ^1H NMR (300 MHz, CDCl_3) δ 1.50 (t, $J=7.0$ Hz, 3H), 4.13 (q, $J=7.0$ Hz, 2H), 6.74 (d, $J=4.3$ Hz, 1H), 6.86 (dd, $J=1.2, 3.7$ Hz, 1H), 6.91 (dd, $J=3.8, 5.1$ Hz, 1H), 7.07 (d, $J=4.3$ Hz, 1H), 7.08 (d, $J=8.9$ Hz, 2H), 7.09 (d, $J=4.7$ Hz, 1H), 7.17 (dd, $J=1.2, 5.1$ Hz, 1H), 7.30 (d, $J=8.9$ Hz, 2H), 7.48 (dd, $J=3.3, 6.2$ Hz, 2H), 7.74 (d, $J=4.5$ Hz, 1H), 7.85 (dd, $J=3.3, 6.2$ Hz, 2H); IR (KBr) 2210, 1496, 1450, 1396, 1362, 1244, 1180, 1163, 1103, 1065, 847 cm^{-1} . Anal. calcd for $2\text{C}_{25}\text{H}_{16}\text{N}_4\text{OS}_2\cdot\text{C}_{10}\text{H}_8$: C, 69.74; H, 3.90; N, 10.84. Found: C, 69.42; H, 4.01; N, 10.77.

4.2.7. 1-(*p*-Ethoxyphenyl)-2-(2-thienyl)-5-[5-(tricyanoethenyl)-2-thienyl]pyrrole-benzothiophene complex (7). Gold-like lustrous crystals; dec (TG-DSC) 158.1°C; ^1H NMR (300 MHz, CDCl_3) δ 1.50 (t, $J=7.0$ Hz, 3H), 4.14 (q, $J=7.0$ Hz, 2H), 6.74 (d, $J=4.3$ Hz, 1H), 6.86 (dd, $J=1.2, 3.7$ Hz, 1H), 6.91 (dd, $J=3.8, 5.1$ Hz, 1H), 7.07 (d, $J=4.3$ Hz, 1H), 7.08 (d, $J=8.9$ Hz, 2H), 7.09 (d, $J=4.7$ Hz, 1H), 7.17 (dd, $J=1.2, 5.1$ Hz, 1H), 7.30 (d, $J=8.9$ Hz, 2H), 7.35 (d, $J=5.7$ Hz, 0.5H), 7.36 (m, 1H), 7.45 (d, $J=5.4$ Hz, 0.5H), 7.74 (d, $J=4.5$ Hz, 1H), 7.83 (m, 0.5H), 7.89 (m, 0.5H); IR (KBr) 2210, 1496, 1450, 1421,

1396, 1362, 1244, 1163, 1105, 1065, 847 cm^{-1} . Anal. calcd for $2\text{C}_{25}\text{H}_{16}\text{N}_4\text{OS}_2\cdot\text{C}_8\text{H}_6\text{S}$: C, 67.03; H, 3.69; N, 10.78. Found: C, 66.96; H, 3.74; N, 10.72.

4.2.8. 1-(*p*-Ethoxyphenyl)-2-(2-thienyl)-5-[5-(tricyanoethenyl)-2-thienyl]pyrrole-anthracene complex (8). Bronze-like lustrous crystals; dec (TG-DSC) 196.6°C; ^1H NMR (300 MHz, CDCl_3) δ 1.50 (t, $J=7.0$ Hz, 3H), 4.14 (q, $J=7.0$ Hz, 2H), 6.74 (d, $J=4.3$ Hz, 1H), 6.86 (dd, $J=1.2, 3.7$ Hz, 1H), 6.90 (dd, $J=3.8, 5.1$ Hz, 1H), 7.07 (d, $J=4.3$ Hz, 1H), 7.08 (d, $J=8.9$ Hz, 2H), 7.09 (d, $J=4.7$ Hz, 1H), 7.17 (dd, $J=1.2, 5.1$ Hz, 1H), 7.30 (d, $J=8.9$ Hz, 2H), 7.47 (dd, $J=3.3, 6.4$ Hz, 2H), 7.73 (d, $J=4.7$ Hz, 1H), 8.01 (dd, $J=3.3, 6.4$ Hz, 2H), 8.43 (s, 1H); IR (KBr) 2208, 1491, 1419, 1396, 1362, 1246, 1163, 1103, 856 cm^{-1} . Anal. calcd for $2\text{C}_{25}\text{H}_{16}\text{N}_4\text{OS}_2\cdot\text{C}_{14}\text{H}_{10}$: C, 70.96; H, 3.91; N, 10.34. Found: C, 70.91; H, 3.97; N, 10.30.

4.2.9. 1-(*p*-Ethoxyphenyl)-2-(2-thienyl)-5-[5-(tricyanoethenyl)-2-thienyl]pyrrole-(phenanthrene)_{0.39}·(anthracene)_{0.11} complex (9). Bronze-like lustrous crystals; dec (TG-DSC) 158.0°C; ^1H NMR (300 MHz, CDCl_3) δ 1.49 (t, $J=7.0$ Hz, 3H), 4.15 (q, $J=7.0$ Hz, 2H), 6.74 (d, $J=4.3$ Hz, 1H), 6.86 (dd, $J=1.2, 3.7$ Hz, 1H), 6.90 (dd, $J=3.8, 5.1$ Hz, 1H), 7.07 (d, $J=4.3$ Hz, 1H), 7.08 (d, $J=8.9$ Hz, 2H), 7.09 (d, $J=4.7$ Hz, 1H), 7.17 (dd, $J=1.2, 5.1$ Hz, 1H), 7.30 (d, $J=8.9$ Hz, 2H), 7.47 (dd, $J=3.3, 6.4$ Hz, 0.44H), 7.58–7.69 (m, 1.56H), 7.73 (d, $J=4.7$ Hz, 1H), 7.75 (s, 0.78H), 7.90 (dd, $J=1.2, 7.5$ Hz, 0.78H), 8.01 (dd, $J=3.3, 6.4$ Hz, 0.44H), 8.43 (s, 0.22H), 8.70 (dd, $J=1.2, 8.1$ Hz, 0.78H); IR (KBr) 2208, 1496, 1450, 1419, 1396, 1362, 1246, 1180, 1163, 1103, 1063, 847 cm^{-1} . Anal. calcd for $2\text{C}_{25}\text{H}_{16}\text{N}_4\text{OS}_2\cdot\text{C}_{14}\text{H}_{10}$: C, 70.96; H, 3.91; N, 10.34. Found: C, 70.75; H, 3.97; N, 10.35.

4.3. X-Ray crystallography

Data collection was performed on a Mac Science MXC18 four-circle diffractometer with graphite monochromated Cu K α radiation ($\lambda=1.54178$ Å) using the θ – 2θ scan technique at 298 K. The structures were solved by direct methods and refined by full-matrix least-squares methods against (SIR 92¹⁵ on a computer program package; maXus ver. 3.2.1 from MAC Science Co. Ltd.). All non-hydrogen atoms were refined with anisotropic displacement parameters and hydrogen atoms were refined isotropically. An empirical absorption correction based on Ψ -scans was only applied to crystal refinements of **6**, **8**, and **9**. Crystallographic data (excluding structure factors) for the structures in this paper have been deposited with the Cambridge Crystallographic Data Centre as supplementary publication numbers CCDC 192045–192051. Copies of the data can be obtained, free of charge, on application to CCDC, 12 Union Road, Cambridge CB2 1EZ, UK (fax: +44-1223-336033 or e-mail: deposit@ccdc.cam.ac.uk).

4.4. Crystal data

Complex **3**: $\text{C}_{27}\text{H}_{20}\text{N}_4\text{O}_2\text{S}_2$, Mr=496.61, gold-like plates, triclinic, space group $P\bar{1}$ (No. 02), $a=8.245(3)$ Å, $b=9.222(6)$ Å, $c=17.333(7)$ Å, $\alpha=75.64(4)^\circ$, $\beta=86.84(3)^\circ$, $\gamma=76.42(4)^\circ$, $V=1241.0(10)$ Å³, $Z=2$, $D_{\text{calcd}}=1.329$ g/cm³, $F(000)=516$, $\mu=2.20$ cm⁻¹; 3982 observed reflections ($I>2\sigma(I)$), 376 parameters, $R=0.080$, $wR=0.083$.

Complex 4: C₂₉H₁₉N₄O₃S₂, Mr=535.69, gold-like plates, triclinic, space group *P* $\bar{1}$ (No. 02), *a*=8.014(2) Å, *b*=9.457(2) Å, *c*=18.384(5) Å, α =102.64(2)°, β =94.92(2)°, γ =104.76(2)°, *V*=1299.7(6) Å³, *Z*=2, *D*_{calcd}=1.369 g/cm³, *F*(000)=554, μ =2.85 cm⁻¹; 4484 observed reflections (*I*>2 σ (*I*)), 404 parameters, *R*=0.062, *wR*=0.086.

Complex 5: C₃₁H₂₁N₄O₂S₂, Mr=529.66, golden yellow plates, triclinic, space group *P* $\bar{1}$ (No. 02), *a*=7.887(3) Å, *b*=9.676(3) Å, *c*=18.913(7) Å, α =97.96(3)°, β =99.92(3)°, γ =106.02(3)°, *V*=1340.0(8) Å³, *Z*=2, *D*_{calcd}=1.313 g/cm³, *F*(000)=550, μ =2.05 cm⁻¹; 4362 observed reflections (*I*>2 σ (*I*)), 392 parameters, *R*=0.065, *wR*=0.079.

Complex 6: C₃₀H₂₀N₄O₂S₂, Mr=516.64, gold-like plates, triclinic, space group *P* $\bar{1}$ (No. 02), *a*=7.796(6) Å, *b*=9.739(4) Å, *c*=18.346(6) Å, α =103.14(3)°, β =93.01(4)°, γ =106.23(4)°, *V*=1292.0(10) Å³, *Z*=2, *D*_{calcd}=1.328 g/cm³, *F*(000)=536, μ =2.11 cm⁻¹; 4551 observed reflections (*I*>1.50 σ (*I*)), 395 parameters, *R*=0.050, *wR*=0.064.

Complex 7: C₅₈H₃₈N₈O₂S₅, Mr=1039.32, gold-like plates, triclinic, space group *P* $\bar{1}$ (No. 02), *a*=7.790(1) Å, *b*=9.714(2) Å, *c*=18.312(4) Å, α =102.93(2)°, β =92.43(2)°, γ =106.02(1)°, *V*=1290.0(4) Å³, *Z*=1, *D*_{calcd}=1.338 g/cm³, *F*(000)=538, μ =2.49 cm⁻¹; 4586 observed reflections (*I*>1.50 σ (*I*)), 398 parameters, *R*=0.056, *wR*=0.063.

Complex 8: C₃₂H₂₁N₄O₂S₂, Mr=541.67, bronze-like rods, triclinic, space group *P* $\bar{1}$ (No. 02), *a*=7.852(1) Å, *b*=9.836(2) Å, *c*=18.669(5) Å, α =97.12(2)°, β =97.44(2)°, γ =107.50(1)°, *V*=1343.1(5) Å³, *Z*=2, *D*_{calcd}=1.339 g/cm³, *F*(000)=562, μ =2.06 cm⁻¹; 4668 observed reflections (*I*>1.50 σ (*I*)), 438 parameters, *R*=0.043, *wR*=0.060.

Complex 9: C₃₂H₂₁N₄O₂S₂, Mr=541.67, bronze-like rods, triclinic, space group *P* $\bar{1}$ (No. 02), *a*=7.838(3) Å, *b*=10.070(3) Å, *c*=18.667(5) Å, α =96.80(2)°, β =98.75(2)°, γ =107.91(2)°, *V*=1364.1(6) Å³, *Z*=2, *D*_{calcd}=1.319 g/cm³, *F*(000)=562, μ =2.03 cm⁻¹; 4271 observed reflections (*I*>2 σ (*I*)), 443 parameters, *R*=0.057, *wR*=0.057.

Acknowledgements

This work was supported by a Grant-in-Aid for Scientific Research (No. 14350464) from the Ministry of Education, Culture, Sports, Science, and Technology of Japan.

References

- For the newest information, trends and prospects in this field, see: (a) Jean-Marie, L. *Science* **2002**, 295, 2400. (b) Reinhoudt, D. N.; Crego-Calama, M. *Science* **2002**, 295, 2403. (c) Olli, I.; Gerrit, T. B. *Science* **2002**, 295, 2407. (d) Mark, D. H. *Science* **2002**, 295, 2410. (e) Takashi, K. *Science* **2002**, 295, 2414. (f) George, M. W.; Bartosz, G. *Science* **2002**, 295, 2418.
- Frederik, C. K.; Mikkil, J. *J. Org. Chem.* **2001**, 66, 6169.
- Ogura, K.; Zhao, R.; Yanai, H.; Maeda, K.; Tozawa, R.; Matsumoto, S.; Akazome, M. *Bull. Chem. Soc. Jpn* **2002**, 75, 2359.
- Zhao, R.; Akazome, M.; Matsumoto, S.; Ogura, K. *Tetrahedron* **2002**, 58, 10225.
- (a) Desiraju, G. R.; Gavezzotti, A. *J. Chem. Soc., Chem. Commun.* **1989**, 621. (b) Gavezzotti, A. *Chem. Phys. Lett.* **1989**, 161, 67. (c) Gavezzotti, A.; Desiraju, G. R. *Acta Crystallogr. sect. B* **1988**, 44, 427.
- For detailed discussions of the aromatic CH– π interaction, see: (a) Lindeman, S. V.; Kosynkin, D.; Kochi, J. K. *J. Am. Chem. Soc.* **1998**, 120, 13268. and the related references listed there. (b) Jorgensen, W. L.; Severance, D. L. *J. Am. Chem. Soc.* **1990**, 112, 4768. (c) Gossel, M. C.; Cheetham, A. K.; Hope, D. A. O.; Weston, S. C. *J. Org. Chem.* **1993**, 58, 6654. and the related references listed there.
- Some information and example on C–H...S interactions, see: (a) Taylor, R.; Kennard, O. *J. Am. Chem. Soc.* **1982**, 104, 5063. (b) Xu, J.; Lai, Y.-H. *Org. Lett.* **2002**, 4, 3211.
- For example, see: (a) Karlström, G.; Linse, P.; Wallqvist, A.; Jönsson, B. *J. Am. Chem. Soc.* **1983**, 105, 3777. (b) Muehldorf, A. V.; Engen, D. V.; Warner, J. C.; Hamilton, A. D. *J. Am. Chem. Soc.* **1988**, 110, 6561. (c) Hobza, P.; Selzle, H. L.; Schlag, E. W. *J. Am. Chem. Soc.* **1994**, 116, 3500. (d) Paliwal, S.; Geib, S.; Wilcox, C. S. *J. Am. Chem. Soc.* **1994**, 116, 4497. (e) Kim, E.-I.; Paliwal, S.; Wilcox, C. S. *J. Am. Chem. Soc.* **1998**, 120, 11192.
- (a) Horner, M. J.; Holman, K. T.; Ward, M. D. *Angew. Chem., Int. Ed.* **2001**, 40, 4045. (b) Akazome, M.; Ueno, Y.; Oiso, H.; Ogura, K. *J. Org. Chem.* **2000**, 65, 68. (c) Akazome, M.; Noguchi, M.; Tanaka, O.; Sumikawa, A.; Uchida, T.; Ogura, K. *Tetrahedron* **1997**, 53, 8315. (d) Ogura, K.; Uchida, T.; Noguchi, M.; Minoguchi, M.; Murata, A.; Fujita, M.; Ogata, K. *Tetrahedron Lett.* **1990**, 31, 3331. (e) Akazome, M.; Yanagita, Y.; Sonobe, R.; Ogura, K. *Bull. Chem. Soc. Jpn* **1997**, 70, 2823.
- For structural analysis of inclusion crystals with mixed guests, see: Caira, M. R.; Nassimbeni, L. R.; Vujovic, D.; Weber, E. *J. Chem. Soc., Perkin Trans. 2* **2001**, 861. and the related reference listed there.
- Apel, S.; Nitsche, S.; Beketov, K.; Seichter, W.; Seidel, J.; Weber, E. *J. Chem. Soc., Perkin Trans. 2* **2001**, 1212.
- A similar result for this phenomenon, see: Caira, M. R.; Nassimbeni, L. R.; Toda, F.; Vujovic, D. *J. Chem. Soc., Perkin Trans. 2* **2001**, 2119.
- For the effect of electrostatic force in aromatic interactions, see: (a) Hunter, C. A.; Lawson, K. R.; Perkins, J.; Urch, C. J. *J. Chem. Soc., Perkin Trans. 2* **2001**, 651. (b) Burini, A.; Fackler, Jr., J. P.; Galassi, R.; Grant, T. A.; Omary, M. A.; Rawashdeh-Omary, M. A.; Pietroni, B. R.; Staples, R. J. *J. Am. Chem. Soc.* **2000**, 122, 11264. (c) Haneline, M. R.; Tsunoda, M.; Gabbai, F. P. *J. Am. Chem. Soc.* **2002**, 124, 3737. (d) Ferguson, S. B.; Diederich, F. *Angew. Chem., Int. Ed. Engl.* **1986**, 25, 1127.
- (a) Ogura, K.; Yanai, H.; Miokawa, M.; Akazome, M. *Tetrahedron Lett.* **1999**, 40, 8887. (b) Yanai, H.; Yoshizawa, D.; Tanaka, S.; Fukuda, T.; Akazome, M.; Ogura, K. *Chem. Lett.* **2000**, 238.
- Altomare, A.; Cascarano, G.; Giacovazzo, C.; Guagliardi, A.; Burla, M. C.; Polidori, G.; Camalli, M. *J. Appl. Crystallogr.* **1994**, 27, 435.